

Contents lists available at ScienceDirect

Icarus

journal homepage: www.elsevier.com/locate/icarus





Widespread pseudo-perennial water ice patches at high northern latitudes on Mars[★]

Colin M. Dundas^{a,*}, Michael T. Mellon^b, Aditya R. Khuller^c, Vidhya Ganesh Rangarajan^d

- ^a U.S. Geological Survey, Astrogeology Science Center, 2255 N. Gemini Dr., Flagstaff, AZ 86001, USA
- ^b Cornell Center for Astrophysics and Planetary Science, Cornell University, Ithaca, NY, USA
- ^c Polar Science Center, Applied Physics Laboratory, University of Washington, Seattle, WA, USA
- ^d Institute of Space Research, German Aerospace Center (DLR), Berlin, Germany

ARTICLE INFO

Keywords: Mars Geological processes Planetary geology Planetary climates

ABSTRACT

The distribution and stability state of Martian water ice deposits are of great interest for understanding recent climate history. Perennial surface ice deposits are rare, but in many regions ice occurs in the subsurface. We observe that summertime meter-scale bright patches are widespread on the plains around the North Polar Layered Deposits. These patches can persist long after disappearance of most seasonal frost but are variable both spatially and year-to-year. These are interpreted as persistent water frost under conditions very near those for perennial surface ice stability. Near this stability point, summer sublimation amounts should be very sensitive to small differences in albedo and thermal inertia, allowing significant variation in the survival time of the patches. Conditions favorable for such pseudo-perennial surface ice are also favorable for current or recent subsurface accumulation. This suggests that the north polar region may be a depositional sink for unstable ice inferred to be receding elsewhere on the planet.

1. Introduction

The distribution and stability of water ice on Mars are of key interest because they are shaped by the climate and thus record its history and current state. Ice is constantly chasing equilibrium as the orbit and climate change, sublimating or depositing as those variations alter the relative stability of different regions. Ice also reshapes the surface geomorphology and is considered a potential habitable environment. Learning the depth and distribution of ice and the controlling processes and transport rates have been identified as critical objectives for Mars science (e.g., Becerra et al., 2021).

Across much of the Martian surface, ice or ice-cemented ground lies beneath a thin layer of dry dust or regolith. (Within this paper, *ice* refers to H_2O ice while CO_2 ice will be specified.) The shallow burial of ice is not an accident: the cover provides thermal protection that reduces the amplitude of temperature variations. The present-day equilibrium depth is estimated to be typically millimeters to centimeters near the poles and up to a few meters in the mid-latitudes, while equatorial ice is unstable at any depth (e.g., Mellon et al., 2004, 2008b; Schorghofer and Aharonson, 2005; Chamberlain and Boynton, 2007).

The main exceptions to the burial of ice are near the north pole. The north polar residual cap (NPRC) is a vast water ice layer at the top of the ice-rich north polar layered deposits (NPLD), mostly located poleward of 80°N (e.g., Byrne, 2009). Crater-filling mounds with exposed ice deposits kilometers in scale are found as far south as Louth crater at 70°N (Brown et al., 2008; Conway et al., 2012). Outlier perennial surface ice deposits hundreds of meters in scale occur as far south as 67°N, generally on cold pole-facing slopes or on the leeward side of some craters (Calvin et al., 2009). In the mid-latitudes, exposures are inherently temporary. Ice excavated by impact craters fades under a sublimation lag within a few years (Dundas et al., 2014). Steep erosional scarps are longer-lived, but only because they are actively retreating and remain unburied due to mass wasting (Dundas et al., 2018; Williams et al., 2022). In the south polar region, perennial surface ice is restricted to a relatively small area poleward of 80°S near the residual CO2 ice cap and is reported to show little or no color or brightness signature at visible wavelengths (e.g., Titus et al., 2003; Bibring et al., 2004; Piqueux et al., 2008). Other than these features, non-polar surface ice occurs as thin, transient deposits that do not persist through the year (e.g., Svitek and Murray, 1990; Carrozzo et al., 2009; Vincendon et al., 2010a; Bapst

E-mail address: cdundas@usgs.gov (C.M. Dundas).

 $^{^{\}star}\,$ This article is part of a Special issue entitled: 'Mars Polar Science' published in Icarus.

^{*} Corresponding author.

et al., 2015; Lange et al., 2024). Below, we refer to all transient seasonal deposits as frost, although some may be deposited as snow (e.g., Whiteway et al., 2009), since it is generally not possible to determine the deposition mechanism in orbital image data.

Surface ice exerts a major influence on the Martian climate. Summer sublimation from the NPRC is a fundamental control on the water vapor abundance in the modern atmosphere (e.g., Jakosky, 1985). In past climate conditions surface ice deposits at other locations could have provided similar controls, and their spatial distribution has important effects on the humidity (e.g., Levrard et al., 2004; Mischna and Richardson, 2005). Perennial surface ice may have been a more widespread feature of the Martian surface in the past. Models for climate scenarios potentially relevant to the last few Myr suggest formation of surface ice deposits at various mid-latitude and equatorial locations (e. g., Mischna et al., 2003; Levrard et al., 2004; Forget et al., 2006; Madeleine et al., 2009, 2014; Steele et al., 2017). Observational evidence exists for past (and sometimes extant, beneath covering layers) ice deposits at some of these sites (e.g., Mustard et al., 2001; Head and Marchant, 2003; Holt et al., 2008; Plaut et al., 2009; Shean, 2010; Bramson et al., 2015; Stuurman et al., 2016). Better knowledge of the nature and behavior of present-day perennial surface ice thus has wider implications for understanding past climate conditions.

The mass balance of extant surface and subsurface ice deposits, an important aspect of their relationship to the modern atmosphere and lower-latitude ice, is the subject of theoretical predictions but has been difficult to determine observationally. Several models suggest that recent conditions should lead to ice accumulation near the north pole (e. g., Levrard et al., 2007; Montmessin et al., 2007; Vos et al., 2019; Mellon and Sizemore, 2022). This is consistent with predictions of currently receding northern mid-latitude ice (e.g., Chamberlain and Boynton, 2007; Mellon and Sizemore, 2022; Vos et al., 2023; Mellon et al., 2024). Mid-latitude ice under level terrain is found equatorward of predicted stable regions (e.g., Mellon et al., 2004; Dundas et al., 2014, 2023; Piqueux et al., 2019; Mellon and Sizemore, 2022); unstable ice is expected to be retreating and must therefore drive deposition somewhere since H₂O is not accumulating in the atmosphere. However, Langevin et al. (2005) reported the appearance of coarse-grained water ice on the NPRC in earlier summer, which they interpreted as older ice being exposed and indicating net sublimation, and Bandfield and Feldman (2008) suggested that shallow thermally derived ice table depths at high latitudes could indicate that the shallow subsurface ice was receding. Other estimates are ambiguous. Ossipian and Brown (2014) noted that ice grain growth could occur over the summer, potentially explaining the observations of Langevin et al. (2005). Brown et al. (2016) reported

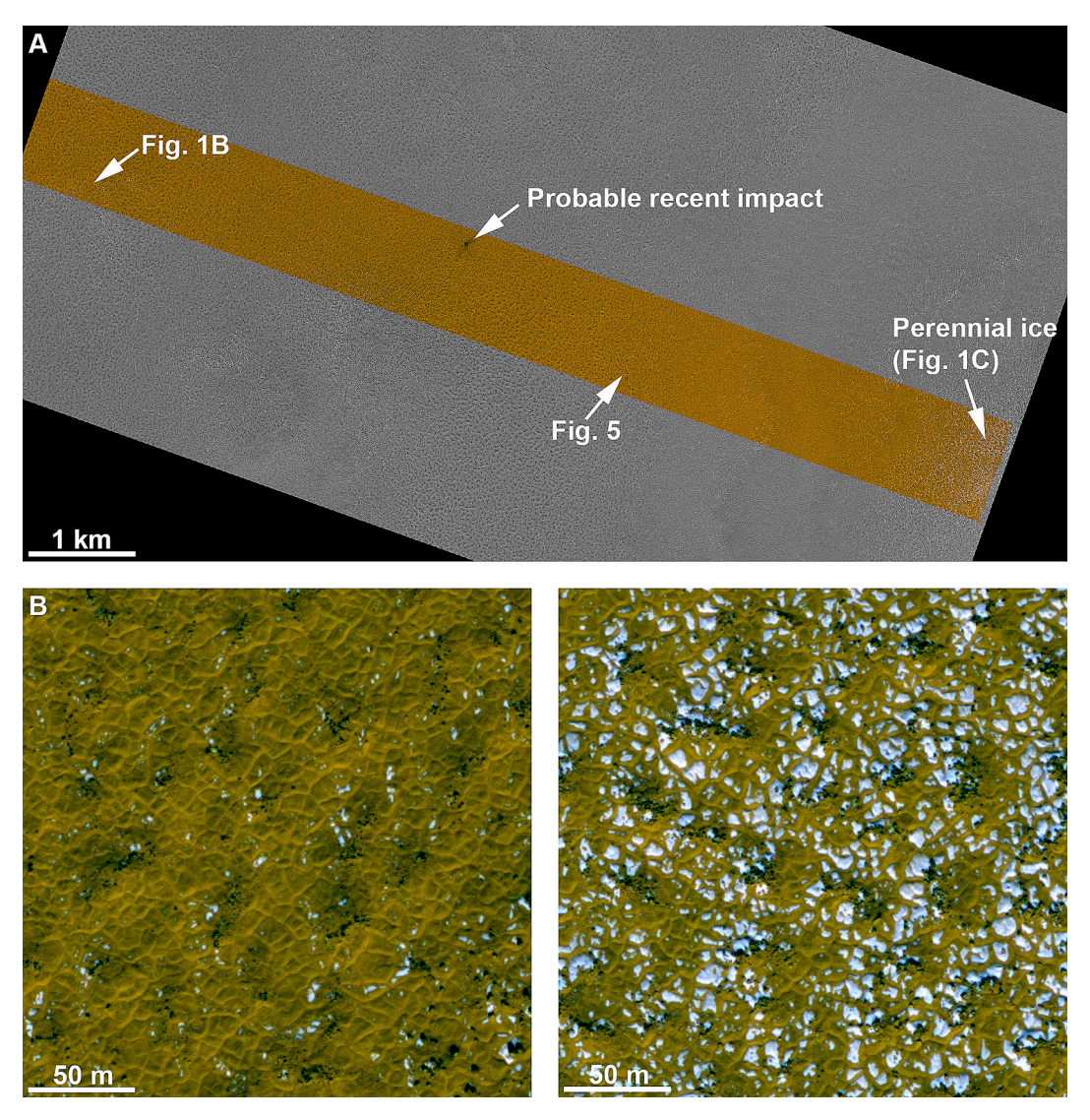


Fig. 1. Example of bright, persistent patches found on flat regolith near 75.4°N, 57.2°E at $L_S = 117^{\circ}$. A) Overview of the location. B) Typical example of bright patches. C) Likely perennial ice deposits on a subtle pole-facing slope. (From HiRISE merged enhanced-color observation ESP_044992_2555 in polar stereographic projection. North is towards the upper left.)

evidence for NPRC accumulation in late summer but did not quantify the annual-net mass budget. Calvin et al. (2015) reported year-to-year variation in NPRC areal coverage but did not find a systematic trend. Modeling of near-polar perennial ice mounds in Louth and Korolev craters suggests that they currently have a net mass balance somewhere between -6 and +2 mm/Mars year (Bapst et al., 2018).

Perennial ice, and particularly changes to perennial ice deposits, are thus key tracers of present-day ice stability and transport. In this manuscript, we describe high-resolution observations of small pseudoperennial ice features observed at high latitudes. We then discuss some theoretical considerations for the occurrence of perennial surface ice. Finally, we discuss the implications of these observations for the recent climate and geomorphology of Mars.

2. Observations of transient summer surface ice

2.1. Survey of high-latitude bright patches

A candidate new impact at 75.4°N noted by Dundas et al. (2021) was surrounded by unusual bright patches extending far beyond the reach of the impact effects, on apparently typical level ground (Fig. 1). These were initially thought to be lingering seasonal frost, but they remained in late-summer images. A similar patch was noted by Kadish and Head (2011). While in any individual image it is difficult to distinguish between small patches of transient frost or perennial ice, year-round persistence is the definition of the difference between the two. Even very small frost patches left behind as seasonal frost recedes typically only linger for a few weeks (e.g., Svitek and Murray, 1990; Gergacz and Kereszturi, 2025).

To understand the distribution and seasonality of such bright patches, we surveyed enhanced-color observations from the High Resolution Imaging Science Experiment (HiRISE; McEwen et al., 2007) with center latitude between 70 and $80^{\circ}N$ and acquisition times between L_S = 90-160°. The latitude bounds were chosen because at the Phoenix landing site (68.2°N, 234.3°E) seasonal frost was gone well before the summer solstice (Cull et al., 2010a, 2010b), while poleward of 80°N the surface is almost exclusively polar layered deposits or the residual H2O ice cap, known to be ice-rich units (e.g., Byrne, 2009). Spot checks indicated that bright patches are rare at latitudes just below 70°N, although not completely absent, so we did not extend the survey further equatorward. The seasonal bounds exclude typical frost, based on regional-scale mapping data, and avoid the onset of thick polar hood clouds. At such regional scales, CO2 frost vanishes at these latitudes between Ls = $40-70^{\circ}$, and H₂O frost is gone at Ls = $70-90^{\circ}$ (e.g., Appéré et al., 2011; Bapst et al., 2015; Piqueux et al., 2015; Khuller et al., 2021). Lange et al. (2024) noted some water ice throughout the summer at high northern latitudes but reported that it was associated with known perennial water ice. The polar hood begins to set in around $L_S=150^{\circ}\,$ (Benson et al., 2011) and HiRISE images are commonly low quality after $L_S = 160^{\circ}$. Images that had excessive atmospheric haze effects were

We surveyed the three-color HiRISE Reduced Data Record (RDR) observations through the summer of Mars Year (MY) 36 (using the Mars Year calendar defined by Clancy et al. (2000)), searching for small spots or patches that were bright and distinctive relative to the adjacent regolith. HiRISE has three color bands (McEwen et al., 2007): near-infrared (IR; center wavelength 874 nm), a broad red filter (RED; center wavelength 694 nm), and blue-green (BG; center wavelength 536 nm), which are assigned to the red, green, and blue channels in color RDRs. Ice-rich material or frost generally appears pale blue or white in stretched HiRISE images. Images were re-stretched as needed for local contrast. We excluded apparent color features that were due to instrument anomalies such as cosmic ray hits and bit-flip artifacts.

The objective of this survey was to examine conditions for typical, roughly level surfaces of apparent regolith material, as distinct from known ice-rich deposits or local pole-facing cold-traps. Thus, we

excluded images that cover only sand dunes or NPLD surfaces and similar materials, but in images with partial coverage by such materials we searched the adjacent sand-free areas within those observations. Within individual images, we also avoided areas that had large steep slopes but searched the entire remaining area, likely including many shallow sloping surfaces. We classified whether bright patches were present or absent; a subset were classified as "fringe" patches when they were near the edge of the NPLD or large icy outliers, and might be partially buried continuations of those units. We did include features gradational with smaller perennial ice deposits like those observed by Seelos et al. (2008) and Calvin et al. (2009) when they transformed into isolated patches on near-level ground. There was substantial ambiguity or gradational boundaries between these classifications. A few examples of bright patches have morphologies suggestive of seasonal frost, such as concentration in polygon troughs where the last seasonal frost is usually observed (cf. Searls et al., 2010), but most do not. We did not exclude bright patches based on such morphologies unless they were obvious transient frost features.

We also conducted the same analysis for 60 images from 70 to $80^{\circ}S$ at $L_S=320{-}330^{\circ},$ distributed at all longitudes and including outcrops of the south PLD (SPLD), but equatorward of the region of known water ice. We did not observe any equivalent bright patches within those observations either on or off the SPLD. As will be seen below, the abundance of such patches in the north is high enough that this sample should have detected them if they behaved similarly in the south.

2.2. Survey results

The survey demonstrated that bright patches are common features all summer throughout most of the study area, although they are rare between \sim 270–350°E (Fig. 2). This distribution is similar to detections of intermediate-sized outlier deposits by Calvin et al. (2009). The patches graded into those deposits where both were present but also occurred in locations with no outlier in the immediate vicinity. The dearth of patches between 270 and 350°E may be due to an anticorrelation between sand dunes and the bright patches. This region corresponds to a wide swath of the polar erg (Hayward et al., 2010), and across the full data set, bright patches were observed in 67 % of images without dunes but only 15 % of images that contained dunes. At local scales, when both occurred together in an image, the patches were usually in the brightest (least sandy) inter-dune areas or outside the dune field. At latitudes below ~72°N, the patches are usually sparse when they do occur. They also appear less common above 76°N after L_S $= 130^{\circ}$ (Fig. 3).

Fig. 4 shows additional examples of patches. At some locations they are concentrated around rocks or on pole-facing micro-slopes, but usually not; concentration around boulders could occur if cold-trapping due to rock shadows were an important process (Svitek and Murray, 1990). Many of the larger examples of patches occur in the level centers of thermal contraction polygons. The patches occur on surfaces both with and without rocks visible at HiRISE resolution. A few occur within relatively light-toned mantling deposits, but this is not common. In examples where dust devil tracks occurred in an image, patches were not notably concentrated along tracks (Fig. 4b), indicating that dust removal by the passing vortex does not create them.

2.3. Case studies

Time series analysis can shed light on the behavior and nature of the bright patches. Here we describe some of the most useful time series and the morphologies of the features.

The best-imaged location for analysis of the patches is the candidate impact location where they were first noted, at 75.4°N, 57.2°E (Figs. 1, 5). The patches were widespread on level ground with scattered boulders, with the largest commonly occurring in the interiors of thermal contraction polygons. Most patches were not associated with boulders.

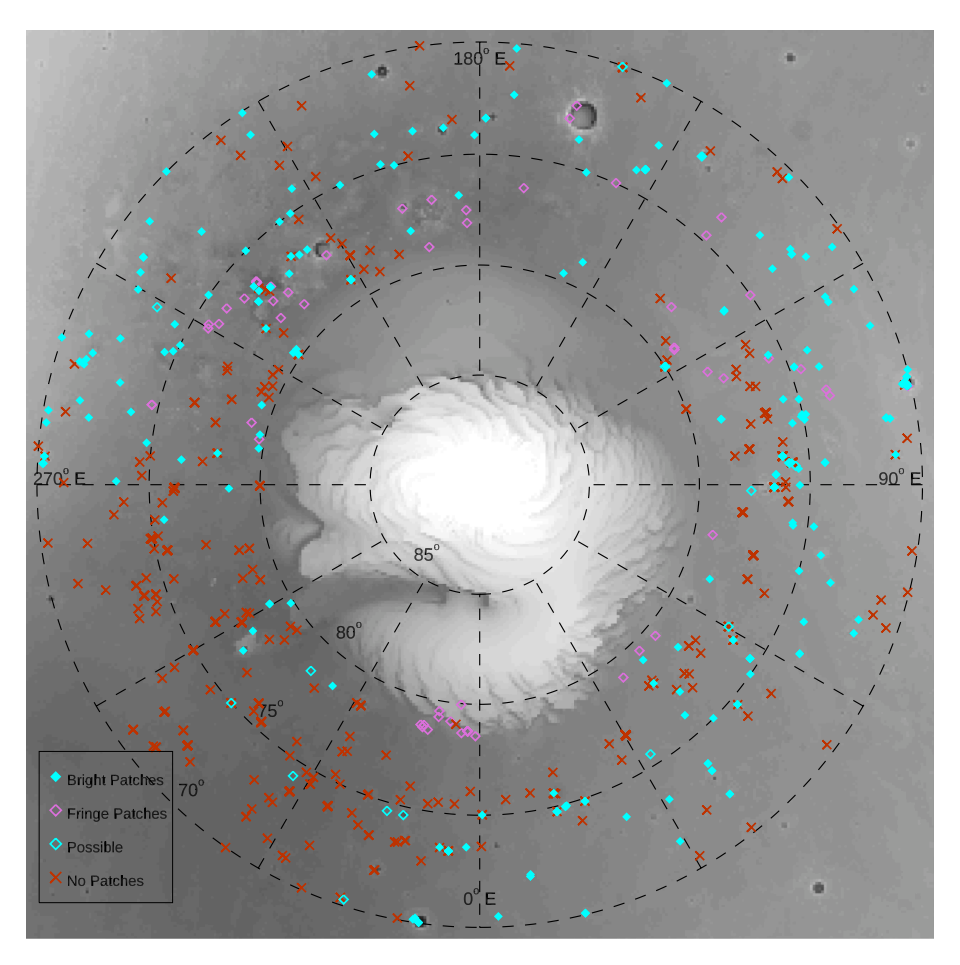


Fig. 2. Polar stereographic map of surveyed HiRISE images with and without bright patches. Mapping was done with HiRISE images between 70 and 80° N. Multiple lines of evidence indicate that the ice table is mostly at 1–10 cm depth in this zone, but somewhat deeper near 310°E than at other longitudes (e.g., Mellon et al., 2008b; Bandfield and Feldman, 2008; Pathare et al., 2018; Piqueux et al., 2019).

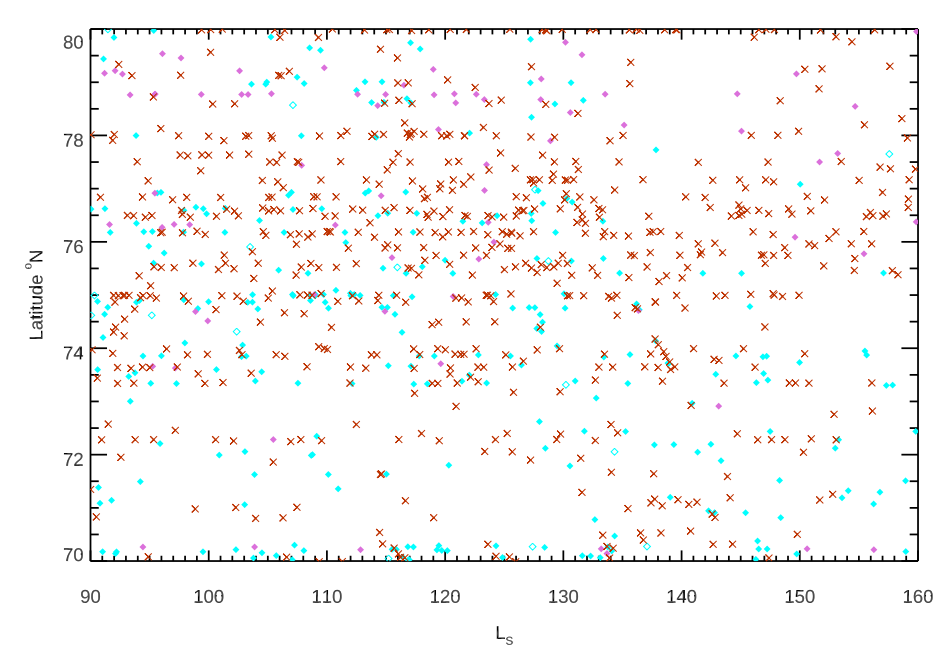


Fig. 3. Timeline showing the time distribution of bright patches in surveyed HiRISE images. Occurrences of bright patches can be found throughout the summer. Legend is the same as in Fig. 2.

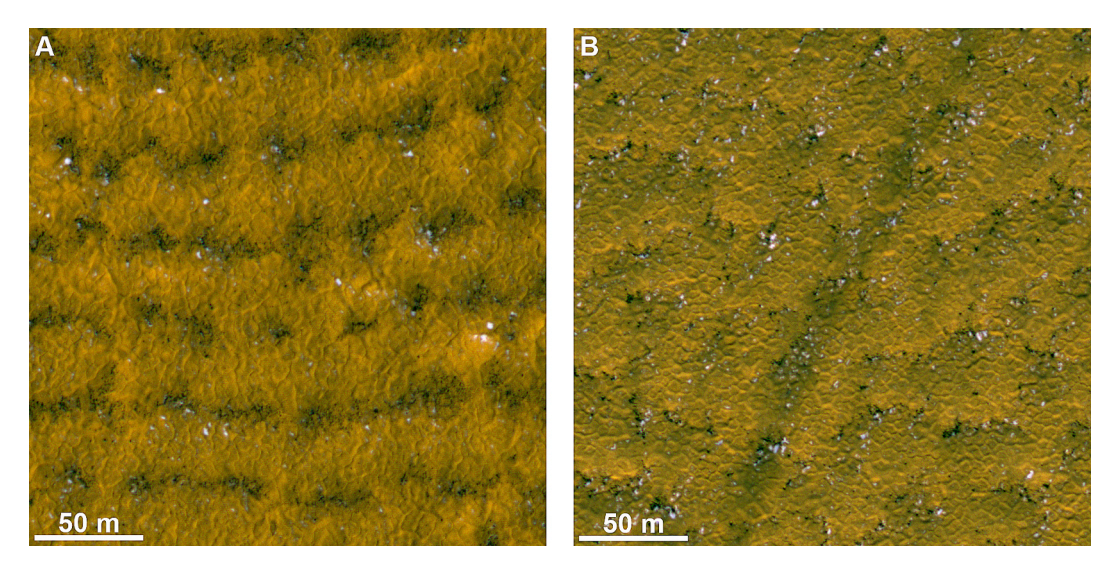


Fig. 4. Additional examples of bright patches. A) Patches among rocky striped ground. Some are associated with rocks and could be influenced by rock shadows, but others are on level ground separated from any topography. B) Patches occur within dust devil tracks (dark band from lower left to upper right) but are not concentrated there. The rubble piles in both A and B may form due to cryoturbation (Mellon et al., 2008a), which could influence the subsurface ice and rock distributions. (Panels are subsections of HiRISE color observations ESP_027148_2525 (A; 72.3°N, 127.2°E) and ESP_027329_2550 (B; 75.0°N, 225.0°E) in polar stereographic projection. Both are stretched individually for maximum color contrast.)

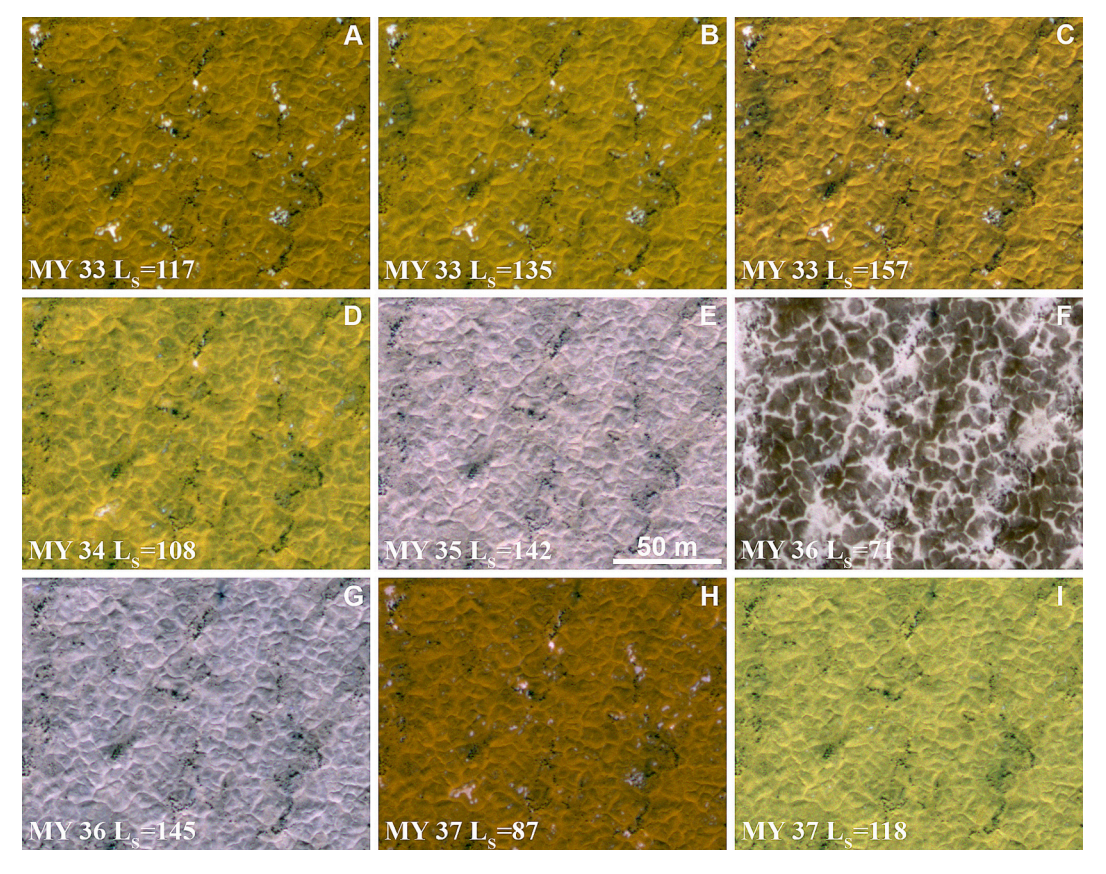


Fig. 5. Time series of images of bright patches near 75.4°N, 57.2°E. The patches persisted through the summer of MY 33 and partially remained in MY 34. They were absent in late summer of MY 35–36. They recurred in MY 37 with approximately the same spatial pattern but did not persist for as long as in MY 33, and have generally disappeared by $L_S = 118^{\circ}$. Center-right panel shows late-spring seasonal frost; major frost concentrations are only loosely correlated with persistent bright patches. (Panels A–I are subsections of HiRISE color observations ESP_044992_2555, ESP_045480_2555, ESP_046047_2555, ESP_053576_2555, ESP_063295_2555, ESP_070128_2555, ESP_072198_2555, ESP_079398_2555, and ESP_079820_2555, respectively, in polar stereographic projection. All images are individually stretched for maximum relative contrast to show the position of the patches, and thus brightness and colors are not comparable between panels. The bland appearance of the MY 35 and 36 summer observations is due to a lack of bright patches, reducing the range of this stretch.)

They occur gradationally in proximity to a likely perennial ice deposit on a shallow pole-facing slope (Fig. 1c); the perennial deposit consists largely of dense-packed patches in polygon centers separated by ice-free lanes along the polygon troughs, and has essentially identical color and brightness characteristics to the smaller patches found kilometers away. The polygons typically have a narrow size range within local areas, but this scale varies spatially in different parts of the image, and the ranges of characteristic polygon sizes for locations on and off the perennial ice deposit overlap. The patches were first observed in the early summer of MY 33 and changed little over the course of the summer, possibly fading slightly (Fig. 5abc). Nearly all of the patches had vanished by early summer of MY 34, but a few remained, and some new examples appeared (Fig. 5d). These patches were absent in the late summer of MY 35 (Fig. 5e); a few possibly recurred in early MY 36 but were absent in a better-quality image acquired later in the summer (Fig. 5g). Once vanished, there was no obvious difference between the location of the patches and nearby regolith in HiRISE data. In early summer of MY 37 widespread patches reappeared, with a spatial distribution that nearly matched their distribution in MY 33 at the sub-meter scale (Fig. 5h), but these largely faded by $L_S = 118^{\circ}$ (Fig. 5i). The perennial ice followed a similar pattern: very distinct in MY 33, incompletely fading in MY35–36 and then somewhat more distinct in early summer of MY37. Some large patches correlate with the location of concentrations of bright, latespring seasonal frost, but others do not, and many large late-spring frost concentrations do not correspond to bright patches (Fig. 5f). The larger perennial ice deposits do appear to correlate with bright, late-

Bright patches at this location and two others were inspected using the multispectral color methods of Rangarajan et al. (2024) (Fig. 6). The color ratios defined therein indicate that the bright patches are not consistent with coarse-grained water ice, but consistent with finer-grained $\rm H_2O$ frost.

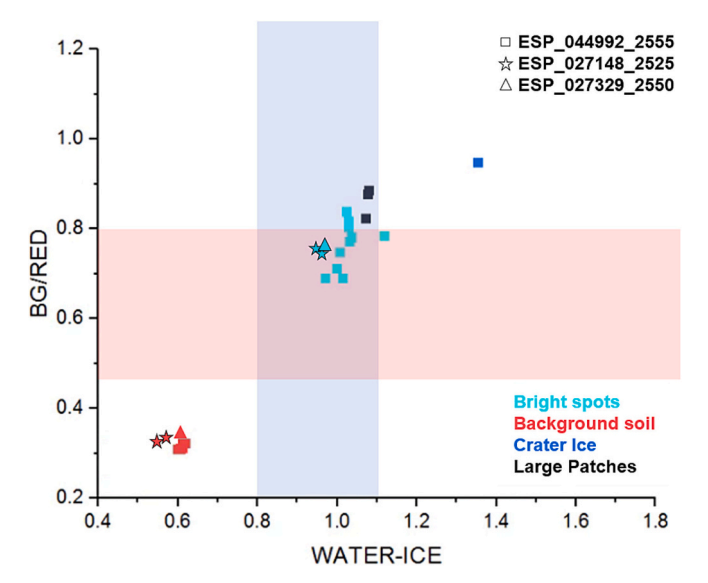


Fig. 6. HiRISE spectral parameter plot of the BG/RED and "WATER-ICE" spectral parameters using shadow correction for atmospheric effects (Rangarajan et al., 2024) showing bright patches, large perennial ice patches, the ice-exposing crater, and the background soil surface, for representative examples from ESP_044992_2555 (Fig. 1) as well as representative bright patches from ESP_027148_2525 and ESP_027329_2550 (Fig. 4). Shaded bands show approximate thresholds for water ice detection with each parameter, based on a suite of examples from many HiRISE images of icy and non-icy features, with points in the upper right quadrant very likely to be near-pure/coarse-grained H₂O ice (Rangarajan et al., 2024). The points plot in a region consistent with but not definitively indicative of water ice, consistent with frost. (For interpretation of the references to color in this figure legend, the reader is referred to the web version of this article.)

A location at 74.8°N, 18.4°E shows evidence for patches reappearing every year from MY 34–36 (Fig. 7a–c). The extent of the patches was different each year but this may be due to different seasonal timing of images, as three images from MY35 demonstrate complete fading over the course of the summer. The patches that did recur were very similar from year to year.

A site at 78.8°N, 212.4°E shows an example of fringe patches near the edge of a perennial ice outlier (Fig. 7d–f). Images at $L_S=104$ – 105° were acquired in MY 29, 31, and 32, and show extremely different patterns, with patches covering a large fraction of the area in MY 31. Although the nature of the bright patches as the fringe of a larger perennial deposit can be seen at large scales, when inspected at full HiRISE resolution the surface looks like normal regolith with thermal contraction polygons.

Louth crater (70.2°N, 103.2°E) shows a diverse array of morphologies. A ~ 10 km diameter ice mound occupies the center of the crater (Brown et al., 2008), surrounded by a darker lithic unit. The surface south of the mound, a shallow pole-facing slope, has abundant patches which are densest adjacent to the ice mound but occur for several km and become abundant again further up the slope. These were classified as fringe patches since the dark unit grades into the ice mound edge. The north side of the mound has a strikingly different morphology, where the ice is overriding dark material with deeper, tens-of-meters-scale polygonal networks along with smaller-scale polygons and with only occasional bright patches. Despite this contrast, the dark material around the edge of the mound is a single continuous unit, even though the ice is burying the dark unit on the north side and gradational with it on the south. This may be a direct consequence of local slope effects on mass balance: Bapst et al. (2018) found that ice on 10° pole-facing slopes could be aggrading while other slopes underwent net loss. Bapst et al. (2018) also inspected HiRISE images and found no changes at the south edge of the mound, but apparent retreat and advance on the north side, possibly due to wind depositing or removing a thin coating of material. We observed more complex behavior for the patches south of the mound: images at similar L_S in different years are quite similar, but patches are systematically less abundant later in the summer when considering the time series as a whole (Fig. 7g-j). This indicates that the patches partially fade over the summer but re-form in identical locations each year prior to summer solstice.

2.4. Interpretation

We considered several hypotheses for the nature of the bright patches. The first is that they are salts, or some other non-icy bright material exposed by the wind. We reject this possibility for several reasons. The patches clearly occur gradationally in proximity to large, definitive surficial water-ice deposits such as that in Louth crater, and to nearby medium-sized deposits where a similar surface-ice interpretation is strongly favored. Some of the latter deposits appear essentially identical in relative color and morphology to a deposit in Heimdal crater with a confirmed spectral signature of water ice (Seelos et al., 2008). When they are observed to change, the patches systematically fade over the summer indicating a volatile composition, while exposures of salts potentially would be both created and buried over time with deposition and removal of surface dust. Inter-annual variability of frost or ice is also more likely than such variability of salts.

A second possibility is that the patches are persistent seasonal CO_2 frost. This can be rejected because it is implausible for CO_2 ice to survive through the summer in unsheltered locations in the northern hemisphere. Although brighter than their surroundings, the albedo of the patches is insufficient to let CO_2 ice persist year-round. The direct input of solar energy should easily remove CO_2 , as occurs regionally by $\text{L}_S = 70^\circ$ at these latitudes (e.g., Appéré et al., 2011; Piqueux et al., 2015; Khuller et al., 2021), well before the end of summer.

A third hypothesis is that the patches represent clean, bright subsurface water ice exposed by wind or seasonal defrosting. While such

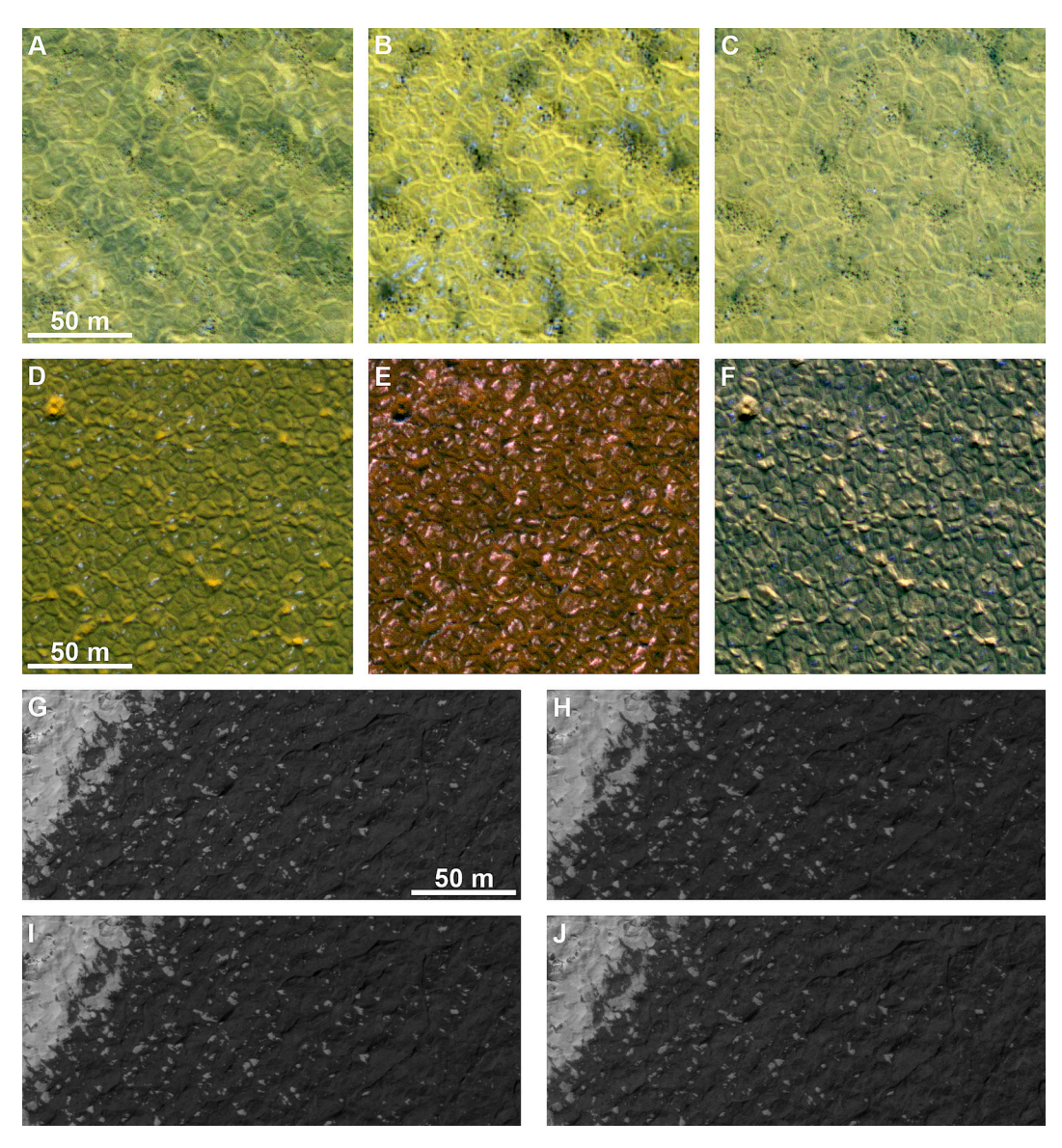


Fig. 7. Image cutouts from time series locations discussed in the text. A–C show images of patches from different Mars years, partially recurring (74.8° N, 18.4° E). The patches are more distinct in B, which is from an earlier L_S than A or C. D—F show a site (78.8° N, 212.4° E) at nearly identical L_S in three different Mars years, demonstrating inter-annual variability. G–J show fringe patches at the edge of the Louth crater ice mound (70.2° N, 103.0° E). The patches are nearly identical at the same L_S in different Mars years (G and I), but are more widespread earlier in the season (H) and less in late summer (J), suggesting that they form similarly year-to-year but fade over the summer each year. (Subsections of HiRISE images in polar stereographic projection. Each has individually been stretched for contrast so colors and brightness are not directly comparable within or between time series. A: ESP_053617_2550, $L_S = 110^\circ$. B: ESP_061978_2550, $L_S = 94^\circ$. C: ESP_071019_2550, $L_S = 104^\circ$. D: PSP_009396_2590, $L_S = 105^\circ$. E: ESP_027026_2590, $L_S = 105^\circ$. F: ESP_035808_2590, $L_S = 104^\circ$. G: PSP_001370_2505, $L_S = 134^\circ$. H: ESP_018301_2505, $L_S = 108^\circ$. I: ESP_019013_2505, $L_S = 134^\circ$. J: ESP_037276_2505, $L_S = 159^\circ$.)

surface erosion may occur in some places, it is unlikely to be a general explanation. If either process were vigorous enough to regularly strip a centimeters-thick dry-regolith layer like that at the Phoenix site (Mellon et al., 2009) over meter-wide areas, they would obscure the well-defined thermal contraction polygon morphologies that are ubiquitous in these regions, which require 10^4 – 10^6 years to form (Sletten et al., 2003). Additionally, extensive regolith erosion by wind transport should long ago have turned mobile regolith into dunes and ripples which are not observed in most bright-patch locations. If the patches formed by exposure of ice from millimeter or shallower depth rather than the expected several cm, they should also concentrate along dust devil tracks formed by removal of surface dust, which is not observed. For either depth scenario, wind erosion and ice exposure should create new patches throughout the summer. However, we have not observed the generation of new patches on this time scale, even though the dunes of

the polar erg are some of the most mobile on Mars (Chojnacki et al., 2019) and must be moving in the summer, the only season when they are frost-free.

A fourth hypothesis for the patches is that they consist of long-lived seasonal $\rm H_2O$ frost. The patches are most distinctive early in the summer after regional frost recession, and new patches do not emerge during the course of the summer, consistent with expectations for frost. The color ratios are also consistent with frost. This frost persistence is qualitatively different from the behavior at even slightly lower latitudes. $\rm H_2O$ frost can only begin to sublimate significantly once underlying $\rm CO_2$ frost is gone (due to the Martian typical $\rm CO_2$ frost point being considerably lower than the typical $\rm H_2O$ frost point), which occurs around $\rm L_S = 40{\text -}70^{\circ}$ for latitudes $\rm 70{\text -}80^{\circ}N$ (Appéré et al., 2011; Piqueux et al., 2015). The $\rm H_2O$ frost then vanishes by around $\rm L_S = 70{\text -}90^{\circ}$ for those latitudes (Appéré et al., 2011; Bapst et al., 2015) so the lifetime is short. Survival

through the summer requires a significant increase in frost longevity, not a modest extension. Additionally, the patches are only partially correlated with the last unambiguous bright seasonal frost (Fig. 5). The patches also do not generally have the small-scale spatial relationships expected for frost: the last bright CO_2 frost concentrates in polygon troughs (Cull et al., 2010a; Searls et al., 2010), but this does not match the distribution of most patches, many of which appear in polygon centers. While some patches occur in plausible cold-trap locations such as local pole-facing slopes, others are on apparently level ground.

These observations are best explained if most of the patches are seasonal H2O frost, but under conditions that are very close to (and grading into) stability of perennial surface ice. The gradation between patches and larger surface water ice deposits favors this pseudoperennial interpretation, and at least some perennial ice displays time variability (fading over multiple years, as at the site in Fig. 1) that is similar to the small patches. The high spatial repeatability of some patches after a multi-year hiatus suggests that they are partially controlled by some persistent feature of the near-surface that is not visible to HiRISE, which could be ground ice that is locally very shallow (perhaps millimeters rather than centimeters). Sufficiently shallow ice will reduce the amplitude of diurnal and seasonal temperature variations due to its high thermal inertia, providing a possible mechanism for localizing frost preservation in places that are not obvious topographic cold traps and allowing partial inter-annual repeatability. The concentration of larger patches in polygon centers is also consistent with the effects of shallow ice playing some role, since observed ice depths at the Phoenix site were greatest in polygon troughs, although observed depths were affected to some extent by regolith mobilized by the descent thrusters (Mellon et al., 2009). The lack of bright patches in the southern hemisphere is consistent with this interpretation, as absolute humidities in the south are generally lower (e.g., Montmessin et al., 2017).

The inter-annual variability of patches at some locations is significant, which could be explained in several ways. First, the frost abundance accumulated each winter could vary. The regional distribution of frost is affected by localized weather fronts during cap recession (cf. Montmessin et al., 2004; Calvin et al., 2015; Titus et al., 2020) which provide a mechanism for variation. Inter-annual variation in CO2 frost abundance could also extend the duration of cold-trapping of water frost. Second, the frost albedo could be affected by a surface dust coating from late-spring dust storms which vary year-to-year. Third, the dust content of the deposited frost could vary inter-annually depending on atmospheric conditions during deposition, producing opaque lags at different times. Finally, wind speed affects sublimation rate and could vary annually (e.g., Martinez et al., 2017). These explanations are not mutually exclusive. A range of conditions must exist in practice: some patches such as those at the fringe of the Louth crater ice mound are truly perennial or nearly so, while others appear to last only partway through the summer or are only persistent in some years.

3. Theoretical considerations for persistent frost and surface ice

The controls on surface ice are somewhat different from those for subsurface ice, and we describe the latter first to clarify the transition between the two. The basic physics controlling subsurface ice have been known for some time (e.g., Leighton and Murray, 1966; Paige, 1992; Mellon and Jakosky, 1993; Mellon et al., 2004; Schorghofer and Aharonson, 2005; Chamberlain and Boynton, 2007). Seasonal and diurnal temperature variations fall with depth. Thus, the annual-mean saturation vapor pressure, which has a non-linear dependence on these temperatures, falls with depth. At some depth temperatures are damped to the point that there is net condensation from atmospheric water vapor. This results in deposition below that transition depth, resulting in an equilibrium ice table. Subsurface ice will aggrade if too deep and recede if too shallow. This is a negative-feedback system: in either case the evolution to the equilibrium depth also drives the net mass flux towards zero and holds it there for as long as the climate conditions remain the

same

Several positive feedback effects also occur that influence the mass balance of shallow-subsurface ice. Surface water frost raises the albedo while it is present; additionally, while sublimating such frost increases the near-surface water-vapor concentration compared with frost-free ground. Both of these effects can increase the stability of underlying subsurface ice (Bapst et al., 2015; Williams et al., 2015); this effect is weak for short-lived mid-latitude frost (Lange et al., 2024) but would be stronger for longer-lived frost. The presence of ground ice raises the thermal inertia of the subsurface, reducing peak temperatures and raising annual-mean temperature (Paige, 1992; Mellon et al., 2004). Additionally, if the ice table is sufficiently shallow, the high thermal inertia of subsurface ice helps to maintain overlying surface water frost for longer intervals by reducing peak surface temperatures, although the stored subsurface heat also reduces the duration of CO2 frost and the lower peak temperatures reduce the efficiency of emitted thermal radiation from the surface, raising mean surface temperature (e.g., Haberle et al., 2008; Vincendon et al., 2010b; Lange et al., 2023). This thermal inertia effect will be important if the ice is significantly shallower than a diurnal skin depth (a few cm for average Martian surface materials). Putzig and Mellon (2007) show that for a stratigraphy of sand or dust over rock (which has a high thermal inertia similar to ice), the apparent thermal inertia in Thermal Emission Spectrometer (TES) data can increase by an order of magnitude as the interface depth decreases from around the diurnal skin depth to negligible, greatly reducing the peak surface temperatures. These feedbacks are mutually reinforcing, and their effects cannot readily be separated: strengthening one has consequences that strengthen the others. As these effects strengthen, they eventually break the negative-feedback system and lead to year-round survival of surface ice, while also raising the subsurface ice table to the surface. All of these effects are strongest for highalbedo, year-round surface ice.

The basic requirement for perennial surface ice persistence or accumulation is that summer sublimation is less than snow precipitation or frost deposition. Potential summer sublimation is extremely sensitive to local conditions. Fig. 8 shows a simple calculation to illustrate the sensitivity of sublimation. The figure shows the calculated net sublimation between $L_S = 90\text{--}135^{\circ}$ using the model of Khuller and Clow (2024) for conditions based on typical atmospheric and surface temperatures and near-surface humidity at high northern latitudes from the Mars Climate Database (MCD; Forget et al., 1999; Millour et al., 2022) and a surface roughness length of 0.1 cm. Relative to the MCD temperatures, the mean temperature is varied up or down (X axis) and the amplitude of diurnal temperature variations is multiplied by a scaling factor (Y axis). These variations serve as a simple proxy for differences in albedo and thermal inertia. Fig. 8a shows that potential sublimation is a strong function of both variables. Changing the mean temperature by 15 K or reducing the diurnal temperature range by a factor of two can reduce potential sublimation by an order of magnitude.

Temperature changes of this order can be induced by changes in albedo and ice table depth. Fig. 9 shows representative calculations from a thermal model (Mellon et al., 2004) demonstrating that for these nearpolar conditions, changes in albedo and associated differences in the equilibrium ice depth have strong effects on the mean temperature and range of variations. The bright patches themselves are likely to exhibit a range of behaviors; they have different annual albedo histories, and the ice table may not be exactly at the present-day equilibrium depth even for a multi-year average albedo, depending on the timescales over which Martian climate has varied.

This sensitivity, rather than specific sublimated thicknesses, is the important result. Sublimation modeling has significant uncertainty, particularly because some input parameters such as near-surface humidity and surface roughness are not well known. Near-polar water frost thicknesses that must survive through the summer are also not observationally well-determined. (To be clearly discernable from orbit, the frost must be optically thick, which Appéré et al. (2011) indicate

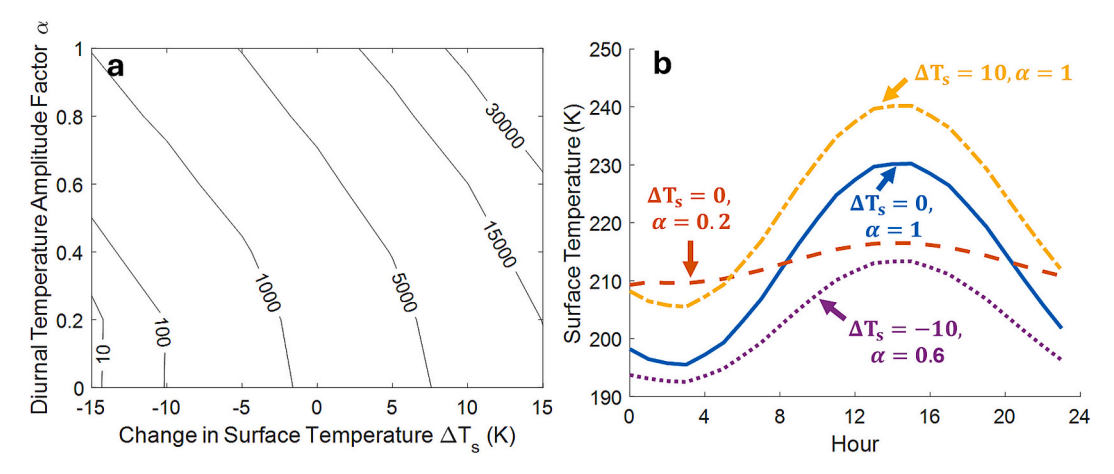


Fig. 8. A) Calculated net sublimated water ice thickness (following Khuller and Clow, 2024) based on surface and air temperatures from the Mars Climate Database (Forget et al., 1999; Millour et al., 2022) at 75°N, 57°E, with offsets to illustrate the sensitivity of sublimation to both mean and peak temperature. Contours show sublimated thickness in microns between $L_S = 90-135^{\circ}$ using a surface roughness length of 0.1 cm. Variation on the X axis offsets mean surface temperature with respect to the MCD baseline value, and on the Y axis reduces the amplitude of diurnal temperature variations by a scaling factor α , thereby reducing peak temperature. Baseline conditions ($\Delta T = 0$, $\alpha = 1$) have sublimation significantly greater than likely frost abundances, but modest reductions in temperature (albedo effects) or diurnal temperature amplitude (thermal inertia effects) reach a regime where survival through much of the summer is plausible. B) Illustration of examples of the temperature offsets applied to create the contour plot in A. The blue curve shows the baseline MCD surface temperature at $L_S = 90^{\circ}$. The yellow curve shows a positive offset in mean temperature ($\Delta T = +10$). The orange curve has a reduced range of diurnal temperatures ($\alpha = 0.2$, so the peak-to-trough temperature difference is only 20 % of the baseline). The purple curve shows an example with both an offset mean and reduced diurnal range. The contours in A were constructed by calculating total sublimation with MCD surface temperatures adjusted by the offsets and amplitude reductions specified on the X and Y axes. (For interpretation of the references to color in this figure legend, the reader is referred to the web version of this article.)

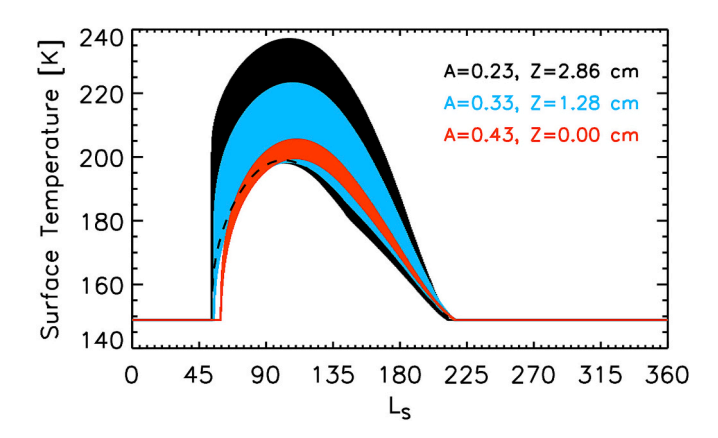


Fig. 9. Temperature calculations for a range of albedos for 75.4°N, for regolith (thermal inertia 250 J m $^{-2}$ K $^{-1}$ s $^{-1/2}$) above ice-cemented ground (thermal inertia 2290 J m $^{-2}$ K $^{-1}$ s $^{-1/2}$) and elevation -2.355 km. The temperatures and associated equilibrium ice table depths are calculated using the model of Mellon et al. (2004). Note that an albedo A=0.43 (similar to that of the large perennial ice mound in Korolev crater) results in an equilibrium ice table depth at the surface (z=0.0). The dashed line shows the lower bound of diurnal temperature variations for A=0.23, which would otherwise be obscured by the other cases.

requires >200 μm total H_2O thickness at near-infrared wavelengths, although this value depends on the H_2O grain size and density (e.g., Wiscombe and Warren, 1980). Brown et al. (2012) suggested late-spring path lengths for light (which they treat as grain size) of 300–1200 μm at high northern latitudes, suggesting that it can have thicknesses at least on that order. If the bright patches locally cold-trap additional frost, they could be substantially thicker than estimates from low-resolution data. However, provided that the surface is near conditions for surface ice persistence, modest variations can easily tip the balance in some years or locations.

Once established (beyond the range of inter-annual variability), surface ice lacks forces that drive it to an equilibrium level at local scales and instead is a neutral- or positive-feedback system. If aggrading, the

surface is regularly adding ice, maintaining the same surface characteristics that allowed it to aggrade. New ice is also likely to be finegrained and thus bright, although accumulation of dusty surface ice is possible. During ice loss, sublimation will generally expose older, coarser-grained, darker ice if sufficient time has passed for grain metamorphism to occur (e.g., Kieffer, 1990; Langevin et al., 2005; Ossipian and Brown, 2014; Brown et al., 2016) and may result in formation of a coating of ice-free lithic material. Thin debris covers will increase the ablation rate by lowering the albedo (observed perennial ice is brighter than most lithic material), until the cover becomes thick enough to act as a diffusive barrier and to damp ice temperature variations (e.g., Leighton and Murray, 1966; Farmer, 1976), transitioning the system to subsurface ice. Whether aggrading or degrading, for surface ice a given set of climate conditions will tend to create a stable accumulation or loss rate rather than a stable surface at outcrop scales. While a state of no net change can occur, this would locally be a coincidental balance with no mechanism holding the system at that state and would be unlikely to persist long or widely. Therefore, if surface ice is visible, it is likely either accumulating, or ablating but being kept relatively clean by erosional processes such as aeolian removal of the sublimation lag. However, regional-scale adjustments like formation or removal of new ice deposits will occur, particularly since the planet-wide distribution of surface ice has a significant effect on the atmospheric water vapor content (e.g., Jakosky, 1985; Mischna and Richardson, 2005).

4. Discussion

The regional distribution of bright patches correlates with other indicators of near-surface $\rm H_2O$, and with the distribution of larger perennial surface ice deposits reported by Calvin et al. (2009). The observed distribution shows that bright patches are widespread except at roughly 270–350°E, where they are less common. Mapping based on near-infrared spectral features has indicated high levels of surface regolith hydration at high northern latitudes, but those levels are reduced in a region centered near 310°E (Audouard et al., 2014; Stcherbinine et al., 2021). Unresolved sub-pixel frost patches could be a factor in creating this spectral signature, although both studies attempted to exclude surface frost. Alternatively, Audouard et al. (2014) suggested that

surface frost could drive enhanced hydration of the regolith, and pseudo-perennial frost would enhance this effect. Analysis of neutron spectrometer data also reveals a lower regional abundance of subsurface hydrogen and greater depth to the hydrogen-rich layer near 310°E (e.g., Pathare et al., 2018). Bandfield and Feldman (2008) used thermal data to estimate extremely shallow ice depths between 70 and 80°N, except for the region around 310°E. They suggested that these extremely shallow ice table depths were close enough to the surface to affect the estimated dry-layer thermal inertia, which would in turn affect the stability of surface frost in places as well.

Although this longitude gap with reduced indications of $\rm H_2O$ and a greater ice table depth near $\rm 310^{\circ}E$ is present in each of the data sets, it may reflect variations in the density of the sand dunes of the polar erg and differences in composition between the dunes and underlying materials. This region has a particularly wide coverage of sand dunes compared with the rest of the $\rm 70{-}80^{\circ}N$ latitude range (Hayward et al., 2010) and vigorous present-day aeolian activity suggests that the dunes themselves have minimal cementing ice (e.g., Hansen et al., 2011; Chojnacki et al., 2019). Dune presence is clearly anticorrelated with the occurrence of local inter-dune bright patches studied here and, if dunes are indeed ice-poor, they would also reduce regional near-infrared, thermal, or neutron ice content signatures. However, inter-dune sand can also darken the albedo, affecting the thermal environment, so the presence of the dunes may also alter conditions for nearby subsurface ice and frost.

Our observations indicate that overall, there are widespread conditions in the region of the bright patches that are very close to those required for perennial surface ice stability, such that net-positive mass balances are not the norm but occur in some years and some places. Locations like that in Fig. 1, where patches are present through the summer in some years but short-lived or absent in others, show that in some years there is a positive net mass balance for surface ice. In other years, bright patches are shorter-lived, indicating either that potential summer sublimation exceeds frost deposition in those years for that site due to inter-annual variations in weather and/or frost properties, or that the patches are optically thin or dustier in those years. Fringe patches in Louth crater also have a range of behaviors: some appear to be truly perennial or nearly so, while others fade under conditions that must be very similar. This again suggests a local range of mass balance conditions, with the distribution varying spatially and from year to year. Thus, conditions across this wide swath of the north polar region are close to those required for net deposition of surface ice and can cross over in

favorable years or settings.

Supporting evidence also points to present-day positive mass balance or very recent accumulation for at least some surface ice deposits. Degrading perennial ice deposits could rapidly bury themselves under an opaque sublimation lag, so they should not remain visible for long. This can be avoided if the lag is removed by the wind, but larger perennial ice deposits are generally on pole-facing or lee slopes (Calvin et al., 2009) rather than those most exposed to aeolian erosion. Additional support for recent accumulation comes from observations of the large perennial ice deposit in the Olympia Mensae region, informally dubbed "Mrs. Chippy's Ring" by Calvin and Titus (2008). Parts of the edge of the bright surface ice appear to be very thin over distances of many kilometers, as the polygonal texture of the underlying material still shows through (Fig. 10), and grades into dense spots and patches, classified as fringe patches here. This suggests that ice in this area has been accumulating very recently, since it is unlikely that degradation of a thicker deposit could produce such an apparently uniform thin veneer draping underlying topography.

The mass balance of subsurface ice deposits is also of interest. Again our observations cannot provide a quantitative measurement but do provide clues. In years or places where frost survives through the year, the subsurface ice mass balance must be positive, or it has reached the surface and is in the process of emerging as surface ice. The range of conditions that permit pseudo-perennial ice would also be favorable for subsurface accumulation, unless it has reached a very shallow equilibrium depth. The exact relationship between the actual and equilibrium ice depth depends on the climate history of Mars, and the relevant conditions can change significantly on timescales as short as decades (e. g., Jakosky, 2024).

Thus, while we cannot establish the current (era of spacecraft observation) net mass balance of the circum-north polar region, our observations are consistent with recent and possibly ongoing surface and subsurface ice accumulation in some near-polar regions. This could provide the depositional sink for ice thought to be retreating elsewhere on the planet.

A corollary of the theories discussed in Section 3 is that formation of a perennial surface ice deposit is likely preceded by the subsurface ice equilibrium depth rising to the surface and the subsurface being infilled by ice in the pores. Conditions where snow and frost have a positive mass balance and persist year-round are almost certainly preceded by a period where they do not survive the entire year, or survive year-round only in some years. In this case, the atmosphere immediately at the

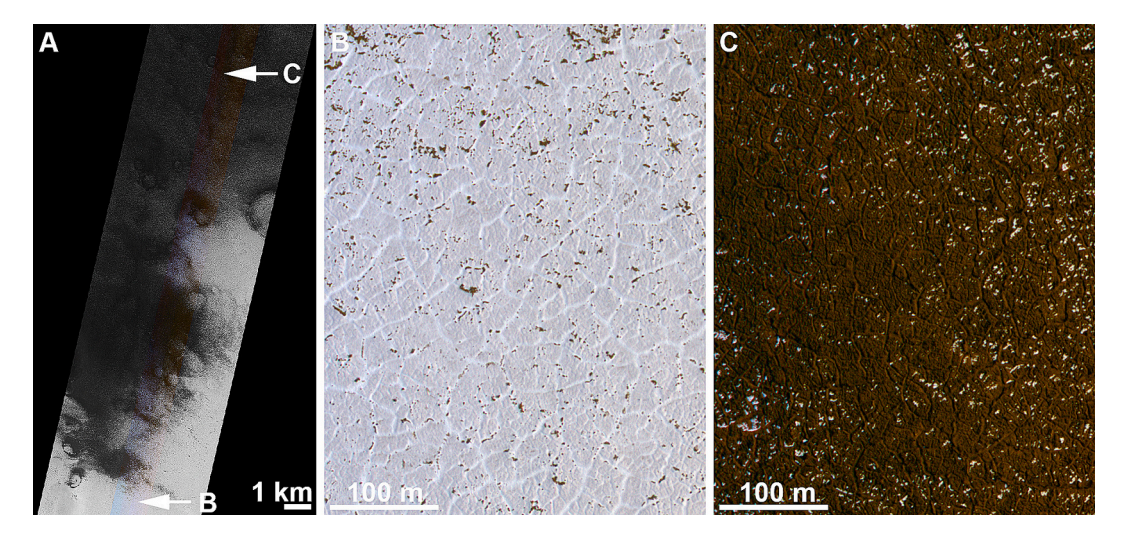


Fig. 10. Apparent thin veneer of surface ice (75°N, 155.7°E). A) Overview of the edge of the deposit. B) Close-up showing a thin coating of bright ice, insufficient to obscure the morphology of polygons. C) View of fringe patches among identical polygons, off the main deposit. The patches grade into continuous cover. (All images are subsections of the merged red-color product for ESP_036285_2550, in polar stereographic projection.) (For interpretation of the references to color in this figure legend, the reader is referred to the web version of this article.)

surface has a water vapor pressure at the surface saturation temperature almost continuously, the equilibrium depth for subsurface ice will be very close to zero, and vapor deposition will fill pores up to that depth. Depending on the sizes of reservoirs, infill of the subsurface could deplete sources before surface accumulation begins. A rapidly changing climate could begin surface accumulation without completely infilling the shallow subsurface, but the regolith pore space beneath that ice would continue to fill in with ice removed from the base of the surface deposit, to a depth determined by the local geothermal gradient (Mellon and Jakosky, 1993). This downward infill process would only be prevented if the surface ice became thick enough that there was no longer a downward-negative gradient in mean water vapor concentration. Diffusion into the subsurface and infill of pore space thus provides an additional loss term even once surface accumulation has started. These effects would reduce surface ice accumulations near the equator or at mid-latitudes relative to model predictions (Jakosky and Carr, 1985; Mischna et al., 2003; Levrard et al., 2004; Forget et al., 2006; Madeleine et al., 2009, 2014; Steele et al., 2017). Additionally, the observations above suggest that the initial formation of surface ice deposits may be patchy.

The edges of surface ice deposits may be locations of particular interest for investigating the present-day astrobiological potential of Mars. High-latitude Martian ice is a potentially habitable environment (e.g., Zent, 2008; Stoker et al., 2010; Mellon et al., 2024). Perchlorate salts, observed at the Phoenix landing site (Hecht et al., 2009), could be produced in the atmosphere (Catling et al., 2010). These salts are considered a possible energy source for any hypothetical microbial life on Mars, as perchlorates are used by some terrestrial bacteria (Stoker et al., 2010). Thin surficial liquid films on ice (Sizemore et al., 2015) could allow movement of soluble materials. Thus, the fringes of a waxing and waning surface ice deposit provide a potential avenue for atmospherically produced species to be transported to subsurface ice that is more protected from radiation.

5. Summary

Small, pseudo-perennial frost patches are widespread at high northern latitudes on Mars. In many cases these patches are gradational with larger, perennial ice deposits. Such pseudo-perennial ice indicates conditions near those required for surface ice stability. This is consistent with current or recent ice accumulation at high northern latitudes, which could be a depositional sink for unstable ice elsewhere on Mars. Although modest changes to the depth of shallow ice will only have small effects on the size of various ice reservoirs, this provides valuable information about which Martian ice deposits are stable or unstable under recent conditions.

CRediT authorship contribution statement

Colin M. Dundas: Writing – review & editing, Writing – original draft, Visualization, Validation, Resources, Project administration, Methodology, Investigation, Funding acquisition, Formal analysis, Data curation, Conceptualization. Michael T. Mellon: Writing – review & editing, Methodology, Investigation, Conceptualization. Aditya R. Khuller: Writing – review & editing, Visualization, Formal analysis. Vidhya Ganesh Rangarajan: Writing – review & editing, Visualization, Formal analysis.

Declaration of competing interest

The authors declare that they have no known competing financial interests or personal relationships that could have appeared to influence the work reported in this paper.

Acknowledgments

We thank Lucas Lange, Glen Cushing, and an anonymous reviewer for helpful comments. CMD was funded by the NASA Mars Data Analysis Program NNH23OB56A. VGR was funded by the Alexander von Humboldt Foundation through a postdoctoral fellowship. HiRISE targeting and imaging were funded by the Mars Reconnaissance Orbiter project. Any use of trade, firm, or product names is for descriptive purposes only and does not imply endorsement by the U.S. Government.

Data availability

Observations of bright patches are available (Dundas, 2025). Image cubes for color analysis are available (Rangarajan, 2025). HiRISE data available via the Planetary Data System (McEwen, 2007).

References

- Appéré, T., Schmitt, B., Langevin, Y., Douté, S., Pommerol, A., Forget, F., Spiga, A., Gondet, B., Bibring, J.-P., 2011. Winter and spring evolution of northern seasonal deposits on Mars from OMEGA on Mars Express. J. Geophys. Res. 116, E05001. https://doi.org/10.1029/2010/E003762.
- Audouard, J., Poulet, F., Vincendon, M., Milliken, R.E., Jouglet, D., Bibring, J.-P., Gondet, B., Langevin, Y., 2014. Water in the Martian regolith from OMEGA/Mars Express. J. Geophys. Res. 119, 1969–1989. https://doi.org/10.1002/2014JE004649.
- Bandfield, J.L., Feldman, W.C., 2008. Martian high-latitude permafrost depth and surface cover thermal inertia distributions. J. Geophys. Res. 113, E08001. https://doi.org/ 10.1029/2007JE003007.
- Bapst, J., Bandfield, J.L., Wood, S.E., 2015. Hemispheric asymmetry in Martian seasonal surface water ice from MGS TES. Icarus 260, 396–408. https://doi.org/10.1016/j. icarus.2015.07.025.
- Bapst, J., Byrne, S., Brown, A.J., 2018. On the icy edge at Louth and Korolev craters. Icarus 308, 15–26. https://doi.org/10.1016/j.icarus.2017.10.004.
- Becerra, P., et al., 2021. Past, present, and future of Mars polar science: outcomes and outlook from the 7th International Conference on Mars Polar Science and Exploration. Planet. Sci. J. 2, 209. https://doi.org/10.3847/PSJ/ac19a5.
- Benson, J.L., Kass, D.M., Kleinböhl, A., 2011. Mars' north polar hood as observed by the Mars Climate Sounder. J. Geophys. Res. 116, E03008. https://doi.org/10.1029/ 2010JE003693.
- Bibring, J.-P., Langevin, Y., Poulet, F., Gendrin, A., Gondet, B., Berthé, M., Soufflot, A., Drossart, P., Combes, M., Bellucci, G., Moroz, V., Mangold, N., Schmitt, B., OMEGA Team, 2004. Perennial water ice identified in the south polar cap of Mars. Nature 428, 627–630. https://doi.org/10.1038/nature02461.
- Bramson, A.M., Byrne, S., Putzig, N.E., Sutton, S., Plaut, J.J., Brothers, T.C., Holt, J.W., 2015. Widespread excess ice in Arcadia Planitia. Mars. Geophys. Res. Lett. 42, 6566–6574. https://doi.org/10.1002/2015GL064844.
- Brown, A.J., Byrne, S., Tornabene, L.L., Roush, T., 2008. Louth crater: evolution of a layered water ice mound. Icarus 196, 433–445. https://doi.org/10.1016/j.icarus 2007.11.023
- Brown, A.J., Calvin, W.M., Murchie, S.L., 2012. Compact Reconnaissance Imaging Spectrometer for Mars (CRISM) north polar springtime recession mapping: first 3 Mars years of observations. J. Geophys. Res. 117, E00J20. https://doi.org/10.1029/ 2012.JE004113
- Brown, A.J., Calvin, W.M., Becerra, P., Byrne, S., 2016. Martian north polar cap summer water cycle. Icarus 277, 401–415. https://doi.org/10.1016/j.icarus.2016.05.007. Byrne, S., 2009. The polar deposits of Mars. Annu. Rev. Earth Planet. Sci. 37, 535–560.
- Byrne, S., 2009. The polar deposits of Mars. Annu. Rev. Earth Planet. Sci. 37, 535–560. https://doi.org/10.1146/annurev.earth.031208.100101.
- Calvin, W.M., Titus, T.N., 2008. Summer season variability of the north residual cap of Mars as observed by the Mars Global Surveyor Thermal Emission Spectrometer (MGS-TES). Planet. Space Sci. 56, 212–226. https://doi.org/10.1016/j. pss.2007.08.005.
- Calvin, W.M., Roach, L.H., Seelos, F.P., Seelos, K.D., Green, R.O., Murchie, S.L., Mustard, J.F., 2009. Compact Reconnaissance Imaging Spectrometer for Mars observations of northern Martian latitudes in summer. J. Geophys. Res. 114, E00D11. https://doi.org/10.1029/2009/E003348.
- Calvin, W.M., James, P.B., Cantor, B.A., Dixon, E.M., 2015. Interannual and seasonal changes in the north polar ice deposits of Mars: observations from MY 29-31 using MARCI. Icarus 251, 181–190. https://doi.org/10.1016/j.icarus.2014.08.026.
- Carrozzo, F.G., Bellucci, G., Altieri, F., D'Aversa, E., Bibring, J.-P., 2009. Mapping of water frost and ice at low latitudes on Mars. Icarus 203, 406–420. https://doi.org/ 10.1016/j.icarus.2009.05.020.
- Catling, D.C., Claire, M.W., Zahnle, K.J., Quinn, R.C., Clark, B.C., Hecht, M.H., Kounaves, S., 2010. Atmospheric origins of perchlorate on Mars and in the Atacama. J. Geophys. Res. 115, E00E11. https://doi.org/10.1029/2009JE003425.
- Chamberlain, M.A., Boynton, W.V., 2007. Response of Martian ground ice to orbit-induced climate change. J. Geophys. Res. 112, E06009. https://doi.org/10.1029/2006JE002801.
- Chojnacki, M., Banks, M.E., Fenton, L.K., Urso, A.C., 2019. Boundary condition controls on the high-sand-flux regions of Mars. Geology 47, 427–430. https://doi.org/ 10.1130/G45793.1.

- Clancy, R.T., Sandor, B.J., Wolff, M.J., Christensen, P.R., Smith, M.D., Pearl, J.C., Conrath, B.J., Wilson, R.J., 2000. An intercomparison of groundbased millimeter, MGS TES, and Viking atmospheric temperature measurements: seasonal and interannual variability of temperatures and dust loading in the global Mars atmosphere. J. Geophys. Res. 105, 9553–9572. https://doi.org/10.1029/ 1000 F601089
- Conway, S.J., Hovius, N., Barnie, T., Besserer, J., Le Mouélic, S., Orosei, R., Read, N.A., 2012. Climate-driven deposition of water ice and the formation of mounds in craters in Mars' north polar region. Icarus 220, 174–193. https://doi.org/10.1016/j. icarus.2012.04.021.
- Cull, S., Arvidson, R.E., Mellon, M., Wiseman, S., Clark, R., Titus, T., Morris, R.V., McGuire, P., 2010a. Seasonal H₂O and CO₂ cycles at the Mars Phoenix landing site: 1. Prelanding CRISM and HiRISE observations. J. Geophys. Res. 115, E00D16. https://doi.org/10.1029/2009JE0033440.
- Cull, S.C., Arvidson, R.E., Morris, R.V., Wolff, M., Mellon, M.T., Lemmon, M.T., 2010b. Seasonal ice cycle at the Mars Phoenix landing site: 2. Postlanding CRISM and ground observations. J. Geophys. Res. 115, E00E19. https://doi.org/10.1029/ 2009 F603410
- Dundas, C.M., 2025. Near-polar bright patches on Mars derived from 2006–2022 HiRISE images. U.S. Geological Survey Data Release. https://doi.org/10.5066/P1OVVDTK.
- Dundas, C.M., Byrne, S., McEwen, A.S., Mellon, M.T., Kennedy, M.R., Daubar, I.J., Saper, L., 2014. HiRISE observations of new impact craters exposing Martian ground ice. J. Geophys. Res. 119, 109–127. https://doi.org/10.1002/2013JE004482.
- Dundas, C.M., Bramson, A.M., Ojha, L., Wray, J.J., Mellon, M.T., Byrne, S., et al., 2018. Exposed subsurface ice sheets in the Martian mid-latitudes. Science 359, 199–201. https://doi.org/10.1126/science.aao1619.
- Dundas, C.M., Mellon, M.T., Conway, S.J., Daubar, I.J., Williams, K.E., Ojha, L., Wray, J. J., Bramson, A.M., Byrne, S., McEwen, A.S., Posiolova, L.V., Speth, G., Viola, D., Landis, M.E., Morgan, G.A., Pathare, A.V., 2021. Widespread exposures of extensive clean shallow ice in the Martian mid-latitudes. J. Geophys. Res. Planets 126, e2020JE006617. https://doi.org/10.1029/2020JE006617.
- Dundas, C.M., Mellon, M.T., Posiolova, L.V., Miljković, K., Collins, G.S., Tornabene, L.L., Rangarajan, V.G., Golombek, M.P., Warner, N.H., Daubar, I.J., Byrne, S., McEwen, A. S., Seelos, K.D., Viola, D., Bramson, A.M., Speth, G., 2023. A large new crater exposes the limits of water ice on Mars. Geophys. Res. Lett. 50, e22GL100747. https://doi. org/10.1029/2022GL100747.
- Farmer, C.B., 1976. Liquid water on Mars. Icarus 28, 279–289. https://doi.org/10.1016/ 0019-1035(76)90038-5.
- Forget, F., Hourdin, F., Fournier, R., Hourdin, C., Talagrand, O., Collins, M., Lewis, S.R., Read, P.L., Huot, J.-P., 1999. Improved general circulation models of the Martian atmosphere from the surface to above 80 km. J. Geophys. Res. 104, 24155–24175. https://doi.org/10.1029/1999JE001025.
- Forget, F., Haberle, R.M., Montmessin, F., Levrard, B., Head, J.W., 2006. Formation of glaciers on Mars by atmospheric precipitation at high obliquity. Science 311, 368–371. https://doi.org/10.1126/science.1120335.
- Gergacz, M., Kereszturi, A., 2025. Survey of remnant seasonal ice patches at southern polar Mars. Icarus 425. https://doi.org/10.1016/j.icarus.2024.116331 article #116331.
- Haberle, R.M., Forget, F., Colaprete, A., Schaeffer, J., Boynton, W.V., Kelly, N.J., Chamberlain, M.A., 2008. The effect of ground ice on the Martian seasonal CO₂ cycle. Planet. Space Sci. 56, 251–255. https://doi.org/10.1016/j.pss.2007.08.006.
- Hansen, C.J., Bourke, M., Bridges, N.T., Byrne, S., Colon, C., Diniega, S., Dundas, C., Herkenhoff, K., McEwen, A., Mellon, M., Portyankina, G., Thomas, N., 2011. Seasonal erosion and restoration of Mars' northern polar dunes. Science 331, 575–578. https://doi.org/10.1126/science.1197636.
- Hayward, R.K., Fenton, L.K., Tanaka, K.L., Titus, T.N., Colaprete, A., Christensen, P.R., 2010. Mars Global Digital Dune Database: MC-1. In: U.S. Geological Survey Open-File Report 2010–1170. https://doi.org/10.3133/ofr20101170.
- Head, J.W., Marchant, D.R., 2003. Cold-based mountain glaciers on Mars: Western Arsia Mons. Geology 31, 641–644. https://doi.org/10.1130/0091-7613(2003)031<0641: CMGOMW>2,0 CO:2
- Hecht, M.H., et al., 2009. Detection of perchlorate and the soluble chemistry of Martian soil at the Phoenix Lander site. Science 325, 64–67. https://doi.org/10.1126/ science.1172466.
- Holt, J.W., et al., 2008. Radar sounding evidence for buried glaciers in the southern midlatitudes of Mars. Science 322, 1235–1238. https://doi.org/10.1126/ science.1164246.
- Jakosky, B.M., 1985. The seasonal cycle of water on Mars. Space Sci. Rev. 41, 131–200. https://doi.org/10.1007/BF00241348.
- Jakosky, B.M., 2024. The present epoch may not be representative in determining the history of water on Mars. Proc. Natl. Acad. Sci. 121, e2321080121. https://doi.org/ 10.1073/nnas.2321080121
- Jakosky, B.M., Carr, M.H., 1985. Possible precipitation of ice at low latitudes of Mars during periods of high obliquity. Nature 315, 559–561. https://doi.org/10.1038/ 315559a0.
- Kadish, S.J., Head, J.W., 2011. Preservation of layered paleodeposits in high-latitude pedestal craters on Mars. Icarus 213, 443–450. https://doi.org/10.1016/j. icarus.2011.03.029.
- Khuller, A.R., Clow, G.D., 2024. Turbulent fluxes and evaporation/sublimation rates on Earth, Mars, Titan, and exoplanets. J. Geophys. Res. 129. https://doi.org/10.1029/ 2023JE008114 article e2023JE008114.
- Khuller, A.R., Christensen, P.R., Harrison, T.N., Diniega, S., 2021. The distribution of frosts on Mars: links to present-day gully activity. J. Geophys. Res. Planets 126. https://doi.org/10.1029/2020JE006577 e2020JE006577.
- Kieffer, H.H., 1990. H₂O grain size and the amount of dust in Mars' residual north polar cap. J. Geophys. Res. 95, 1481–1493. https://doi.org/10.1029/JB095iB02p01481.

Lange, L., Forget, F., Vincendon, M., Spiga, A., Vos, E., Aharonson, O., Millour, E., Bierjon, A., Vandemeulebrouck, R., 2023. A reappraisal of subtropical subsurface water ice stability on Mars. Geophys. Res. Lett. 50, e2023GL105177. https://doi.org/10.1029/2023GL105177

- Lange, L., Piqueux, S., Edwards, C.S., Forget, F., Naar, J., Vos, E., Szantai, A., 2024. Observations of water frost on Mars with THEMIS: application to the presence of brines and the stability of (sub)surface water ice. J. Geophys. Res. Planets 129, e2024JE008489. https://doi.org/10.1029/2024JE008489.
- Langevin, Y., Poulet, F., Bibring, J.-P., Schmitt, B., Douté, S., Gondet, B., 2005. Summer evolution of the north polar cap of Mars as observed by OMEGA/Mars Express. Science 307, 1581–1584. https://doi.org/10.1126/science.1109438.
- Leighton, R.B., Murray, B.C., 1966. Behavior of carbon dioxide and other volatiles on Mars. Science 153, 136–144. https://doi.org/10.1126/science.153.3732.136.
- Levrard, B., Forget, F., Montmessin, F., Laskar, J., 2004. Recent ice-rich deposits formed at high latitudes on Mars by sublimation of unstable equatorial ice during low obliquity. Nature 431, 1072–1075. https://doi.org/10.1038/nature03055.
- Levrard, B., Forget, F., Montmessin, F., Laskar, J., 2007. Recent formation and evolution of northern Martian polar layered deposits as inferred from a Global Climate Model. J. Geophys. Res. 112, E06012. https://doi.org/10.1029/2006JE002772.
- Madeleine, J.-B., Forget, F., Head, J.W., Levrard, B., Montmessin, F., Millour, E., 2009. Amazonian northern mid-latitude glaciation on Mars: a proposed climate scenario. Icarus 203, 390–405. https://doi.org/10.1016/j.icarus.2009.04.037.
- Madeleine, J.-B., Head, J.W., Forget, F., Navarro, T., Millour, E., Spiga, A., Colaïtis, A., Määttänen, A., Montmessin, F., Dickson, J.L., 2014. Recent ice ages on Mars: the role of radiatively active clouds and cloud microphysics. Geophys. Res. Lett. 41, 4873–4879. https://doi.org/10.1002/2014GL059861.
- Martinez, G.M., et al., 2017. The modern near-surface Martian climate: a review of insitu meteorological data from Viking to Curiosity. Space Sci. Rev. 212, 295–338. https://doi.org/10.1002/s11214-017-0360-x.
- McEwen, A., 2007. Mars Reconnaissance Orbiter High Resolution Imaging Science Experiment, Reduced Data Record, MRO-M-HIRISE-3-RDR-V1.1, NASA Planetary Data System. https://doi.org/10.17189/1520303.
- McEwen, A.S., Eliason, E.M., Bergstrom, J.W., Bridges, N.T., Hansen, C.J., Delamere, W. A., Grant, J.A., Gulick, V.C., Herkenhoff, K.E., Keszthelyi, L., Kirk, R.L., Mellon, M.T., Squyres, S.W., Thomas, N., Weitz, C.M., 2007. Mars reconnaissance orbiter's high resolution imaging science experiment (HiRISE). J. Geophys. Res. 112, E05S02. https://doi.org/10.1029/2005JE002605.
- Mellon, M.T., Jakosky, B.M., 1993. Geographic variations in the thermal and diffusive stability of ground ice on Mars. J. Geophys. Res. 98, 3345–3364. https://doi.org/ 10.1029/92JE02355.
- Mellon, M.T., Sizemore, H.G., 2022. The history of ground ice at Jezero Crater Mars and other past, present, and future landing sites. Icarus 371. https://doi.org/10.1016/j. icarus.2021.114667 article #114667.
- Mellon, M.T., Feldman, W.C., Prettyman, T.H., 2004. The presence and stability of ground ice in the southern hemisphere of Mars. Icarus 169, 324–340. https://doi. org/10.1016/j.icarus.2003.10.022.
- Mellon, M.T., Arvidson, R.E., Marlow, J.J., Phillips, R.J., Asphaug, E., 2008a. Periglacial landforms at the Phoenix landing site and the northern plains of Mars. J. Geophys. Res. 113, E00A23. https://doi.org/10.1029/2007JE003039.
- Mellon, M.T., Boynton, W.V., Feldman, W.C., Arvidson, R.E., Titus, T.N., Bandfield, J.L., Putzig, N.E., Sizemore, H.G., 2008b. A prelanding assessment of the ice table depth and ground ice characteristics in Martian permafrost at the Phoenix landing site. J. Geophys. Res. 113, E00A25. https://doi.org/10.1029/2007JE003067.
- Mellon, M.T., Arvidson, R.E., Sizemore, H.G., Searls, M.L., Blaney, D.L., Cull, S., et al., 2009. Ground ice at the Phoenix landing site: stability state and origin. J. Geophys. Res. 114, E00E07. https://doi.org/10.1029/2009JE003417.
- Mellon, M.T., Sizemore, H.G., Heldmann, J.L., McKay, C.P., Stoker, C.R., 2024. The habitability conditions of possible Mars landing sites for life exploration. Icarus 408. https://doi.org/10.1016/j.icarus.2023.115836 article #115836.
- Millour, E., et al., 2022. The Mars Climate Database (version 6.1). 16th Europlanet Science Congress, abstract EPSC2022-786. https://doi.org/10.5194/epsc2022-786
- Mischna, M.A., Richardson, M.I., 2005. A reanalysis of water abundances in the Martian atmosphere at high obliquity. Geophys. Res. Lett. 32, L03201. https://doi.org/10.1029/2004GL021865.
- Mischna, M.A., Richardson, M.I., Wilson, R.J., McCleese, D.J., 2003. On the orbital forcing of Martian water and CO₂ cycles: a general circulation model study with simplified volatile schemes. J. Geophys. Res. 108, 5062. https://doi.org/10.1029/ 2003JE002051.
- Montmessin, F., Forget, F., Rannou, P., Cabane, M., Haberle, R.M., 2004. Origin and role of water ice clouds in the Martian water ice cycle as inferred from a general circulation model. J. Geophys. Res. 109, E10004. https://doi.org/10.1029/ 2004.F002284
- Montmessin, F., Haberle, R.M., Forget, F., Langevin, Y., Clancy, R.T., Bibring, J.-P., 2007. On the origin of perennial water ice at the south pole of Mars: a precession-controlled mechanism? J. Geophys. Res. 112, E08S17. https://doi.org/10.1029/ 2007/E002002
- Montmessin, F., Smith, M.D., Langevin, Y., Mellon, M.T., Fedorova, A., 2017. The water cycle. In: Haberle, R.M., et al. (Eds.), The Atmosphere and Climate of Mars, pp. 338–373. https://doi.org/10.1017/9781139060172.011. Cambridge, 2017.
- Mustard, J.F., Cooper, C.D., Rifkin, M.K., 2001. Evidence for recent climate change on Mars from the identification of youthful near-surface ground ice. Nature 412, 411–414. https://doi.org/10.1038/35086515.
- Ossipian, S., Brown, A.J., 2014. How fast can water ice grains grow on the summertime Martian north pole?. In: 8th Int. Conf. Mars, abstract #1071.
- Paige, D.A., 1992. The thermal stability of near-surface ground ice on Mars. Nature 356, 43–45. https://doi.org/10.1038/356043a0.

- Pathare, A.V., Feldman, W.C., Prettyman, T.H., Maurice, S., 2018. Driven by excess? Climatic implications of new global mapping of near-surface water-equivalent hydrogen on Mars. Icarus 301, 97–116. https://doi.org/10.1016/j. icarus.2017.09.031.
- Piqueux, S., Edwards, C.S., Christensen, P.R., 2008. Distribution of the ices exposed near the south pole of Mars using Thermal Emission Imaging System (THEMIS) temperature measurements. J. Geophys. Res. 113, E08014. https://doi.org/ 10.1029/2007JE003055.
- Piqueux, S., Kleinböhl, A., Hayne, P.O., Kass, D.M., Schofield, J.T., McCleese, D.J., 2015.
 Variability of the Martian seasonal CO₂ cap extent over eight Mars Years. Icarus 251, 164–180. https://doi.org/10.1016/j.icarus.2014.10.045.
- Piqueux, S., Buz, J., Edwards, C.S., Bandfield, J.L., Kleinböhl, A., Kass, D.M., Hayne, P.O., the MCS and THEMIS teams, 2019. Widespread shallow water ice on Mars at high latitudes and mid latitudes. Geophys. Res. Lett. 46, 14290–14298. https://doi.org/ 10.1029/2019GL083947.
- Plaut, J.J., Safaeinili, A., Holt, J.W., Phillips, R.J., Head, J.W., Seu, R., Putzig, N.E., Frigeri, A., 2009. Radar evidence for ice in lobate debris aprons in the mid-northern latitudes of Mars. Geophys. Res. Lett. 36, L02203. https://doi.org/10.1029/ 2008GL036379.
- Putzig, N.E., Mellon, M.T., 2007. Apparent thermal inertia and the surface heterogeneity of Mars. Icarus 191, 68–94. https://doi.org/10.1016/j.icarus.2007.05.013.
- Rangarajan, V.G., 2025. Data for: "Widespread Pseudo-Perennial Water Ice Patches at High Northern Latitudes on Mars". Zenodo. https://doi.org/10.5281/ zenodo.15263647.
- Rangarajan, V.G., et al., 2024. Novel quantitative methods to enable multispectral identification of high-purity water ice exposures on Mars using High Resolution Imaging Science Experiment (HiRISE) images. Icarus 419. https://doi.org/10.1016/ j.icarus.2023.115849 article #115849.
- Schorghofer, N., Aharonson, O., 2005. Stability and exchange of subsurface ice on Mars. J. Geophys. Res. 110, E05003. https://doi.org/10.1029/2004JE002350.
- Searls, M.L., Mellon, M.T., Cull, S., Hansen, C.J., Sizemore, H.G., 2010. Seasonal defrosting of the Phoenix landing site. J. Geophys. Res. 115, E00E24. https://doi. org/10.1029/2009JE003438.
- Seelos, K.D., Arvidson, R.E., Cull, S.C., Hash, C.D., Heet, T.L., Guinness, E.A., McGuire, P. C., Morris, R.V., Murchie, S.L., Parker, T.J., Roush, T.L., Seelos, F.P., Wolff, M.J., 2008. Geomorphic and mineralogical characterization of the northern plains of Mars at the Phoenix Mission candidate landing sites. J. Geophys. Res. 113, E00A13. https://doi.org/10.1029/2008JE003088.
- Shean, D.E., 2010. Candidate ice-rich material within equatorial craters on Mars. Geophys. Res. Lett. 37, L24202. https://doi.org/10.1029/2010GL045181.
- Sizemore, H.G., Zent, A.P., Rempel, A.W., 2015. Initiation and growth of Martian ice lenses. J. Icarus 251, 191–210. https://doi.org/10.1016/j.jcarus.2014.04.013.
- Sletten, R.S., Hallet, B., Fletcher, R.C., 2003. Resurfacing time of terrestrial surfaces by the formation and maturation of polygonal patterned ground. J. Geophys. Res. 108, 8044. https://doi.org/10.1029/2002JE001914.
- Stcherbinine, A., Vincendon, M., Montmessin, F., Beck, P., 2021. Identification of a new spectral signature at 3 µm over Martian northern high latitudes: implications for

- surface composition. Icarus 369. https://doi.org/10.1016/j.icarus.2021.114627 article #114627.
- Steele, L.J., Balme, M.R., Lewis, S.R., 2017. Regolith-atmosphere exchange of water in Mars' recent past. Icarus 284, 233–248. https://doi.org/10.1016/j. icarus 2016.11.023
- Stoker, C.R., Zent, A., Catling, D.C., Douglas, S., Marshall, J.R., Archer, D., Clark, B., Kounaves, S.P., Lemmon, M.T., Quinn, R., Renno, N., Smith, P.H., Young, S.M.M., 2010. Habitability of the Phoenix landing site. J. Geophys. Res. 115, E00E20. https://doi.org/10.1029/2009JE003421.
- Stuurman, C.M., Osinski, G.R., Holt, J.W., Levy, J.S., Brothers, T.C., Kerrigan, M., Campbell, B.A., 2016. SHARAD detection and characterization of subsurface water ice deposits in Utopia Planitia. Mars. Geophys. Res. Lett. 43, 9484–9491. https://doi.org/10.1002/2016GL070138.
- Svitek, T., Murray, B., 1990. Winter frost at Viking Lander 2 site. J. Geophys. Res. 95, 1495–1510. https://doi.org/10.1029/JB095iB02p01495.
- Titus, T.N., Kieffer, H.H., Christensen, P.R., 2003. Exposed water ice discovered near the south pole of Mars. Science 299, 1048–1051. https://doi.org/10.1126/science.1080497.
- Titus, T.N., Williams, K.E., Cushing, G.E., 2020. Conceptual model for the removal of cold-trapped H2O ice on the Mars northern seasonal springtime polar cap. Geophys. Res. Lett. 47, e2020GL087387. https://doi.org/10.1029/2020GL08738.
- Vincendon, M., Forget, F., Mustard, J., 2010a. Water ice at low to midlatitudes on Mars. J. Geophys. Res. 115, E10001. https://doi.org/10.1029/2010JE003584.
- Vincendon, M., Mustard, J., Forget, F., Kreslavsky, M., Spiga, A., Murchie, S., Bibring, J.-P., 2010b. Near-tropical subsurface ice on Mars. Geophys. Res. Lett. 37, L01202. https://doi.org/10.1029/2009GL041426.
- Vos, E., Aharonson, O., Schorghofer, N., 2019. Dynamic and isotopic evolution of ice reservoirs on Mars. Icarus 324, 1–7. https://doi.org/10.1016/j.icarus.2019.01.018.
- Vos, E., Aharonson, O., Schörghofer, N., Forget, F., Lange, L., Millour, E., 2023. Paleo-evolution of Martian subsurface ice and its role in the polar physical and isotopic layering. J. Geophys. Res. 128, e2023JE007822. https://doi.org/10.1029/2023JE007822.
- Whiteway, J.A., et al., 2009. Martian water-ice clouds and precipitation. Science 325, 68–70. https://doi.org/10.1126/science.1172344.
- Williams, K.E., McKay, C.P., Heldmann, J.L., 2015. Modeling the effects of martian surface frost on ice table depth. Icarus 261, 58–65. https://doi.org/10.1016/j. icarus.2015.08.005.
- Williams, K.E., Dundas, C.M., Kahre, M.A., 2022. The formation mechanisms for midlatitude ice scarps on Mars. Icarus 386. https://doi.org/10.1016/j. icarus.2022.115174 article #115174.
- Wiscombe, W.J., Warren, S.G., 1980. A model for the spectral albedo of snow. I: pure snow. J. Atmos. Sci. 37, 2712–2733. https://doi.org/10.1175/1520-0469(1980) 037<2712;AMFTSA>2.0.CO;2.
- Zent, A., 2008. A historical search for habitable ice at the Phoenix landing site. Icarus 196, 385–408. https://doi.org/10.1016/j.icarus.2007.12.028.